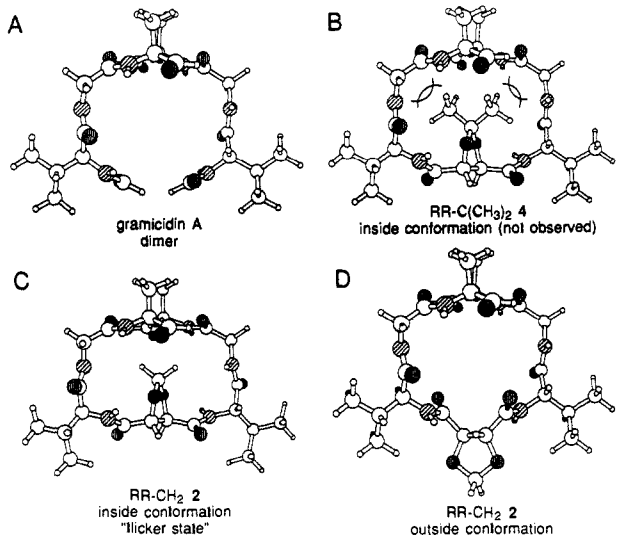

Figure 4. Top view through the central turn of the channel helix including the linker (for comparison, natural gA is also shown): (A) natural gA with no linker, (D) the linker ring of **2** outside and (C) inside the pore. The bulkier ring of **4** cannot be accommodated inside the channel pore (B) and suffers severe steric strain in the inside–outside transition (diagram not provided).

dimers. Note that each upward rise indicates a channel opening and represents the ion flux through a *single molecule* of the dimer. Each dimer exhibited very long open-channel lifetimes (>30 min). Under identical conditions, gA channels have a lifetime of 10–120 s. Both *S,S* dimers **1** and **3** have conductances similar to that of gA, whereas the conductances of the *R,R* dimers **2** and **4** in KCl (Figure 2A) are lower than those of the *S,S* dimers. In HCl solutions the conductances of all the dimers, as well as of gA, are nearly the same (Figure 2B). These latter observations are readily explained by the Grotthus mechanism of proton conductance mentioned above. While proton conductance is sensitive to a complete blockage of the channel, it is not very sensitive to structural distortions along the channel as long as the water chain inside the channel remains intact. The conductance of alkali ions, however, is expected to be susceptible to even minor steric disturbances, due to the attendant effect on the solvation of the ion as it passes through the channel. Whereas both *S,S* dimers exhibit a linear current–voltage (*iV*) relationship, both *R,R* (mismatched) dimers exhibit a hyperlinear current–voltage relationship (data not shown). These results also indicate that the *R,R* dimers have a disturbance at the center of the channel.[8]

A clear distinction between the *R,R* dimers **2** and **4** can be seen in the traces shown in Figure 2B. The RR-$C(CH_3)_2$ dimer **4** does not exhibit the flickering behavior found in the RR-CH_2 dimer **2** (Figure 3). This result provides support for our hypothesis that the flickers are caused by the flipping of the dioxolane ring of **2** into and out of the channel since the dioxolane ring in the RR-$C(CH_3)_2$ dimer **4** is expected to be too large to either fit inside the channel (see Figure 4) or undergo the inside–outside transition. This study represents one step toward a detailed understanding of the dynamic properties of artificial channel molecules such as **2**. An increased understanding of gating mechanisms is hoped to facilitate the rational design of control elements for the gating of transmembrane ion channels.[9]

Acknowledgment. S.H.H. was supported by a stipend of the Max-Planck-Gesellschaft. S.L.S. is pleased to acknowledge the NIGMS for generous support and Pfizer, Inc., for a graduate fellowship (awarded to C.J.S.). We thank Professor M. Karplus and B. Roux for the coordinates of the gA helix dimers, Dr. G. Glick and B. Roux for helpful suggestions regarding molecular modeling, Professors E. Neher and F. J. Sigworth for support of S.H.H., and Dr. W. McMurray (Mass Spectrometry Facility at the Yale Comprehensive Cancer Center).

(8) This conclusion is based on a formalism describing the ion transport by migration of ions through an energy profile with two minima and three barriers. See ref 2.

(9) See also: (A) Lear, J. D.; Wasserman, Z. R.; DeGrado, W. F. *Science* **1988**, *240*, 1177. (b) Carmicheal, V. E.; Dutton, P. J.; Fyles, T. M.; James, T. D.; Swan, J. A.; Zojaji, M. *J. Am. Chem. Soc.* **1989**, *111*, 767. (c) Jullien, L.; Lehn, J.-M. *Tetrahedron Lett.* **1988**, *29*, 3803 and references therein.

Phospholipase A_2 Engineering. 3. Replacement of Lysine-56 by Neutral Residues Improves Catalytic Potency Significantly, Alters Substrate Specificity, and Clarifies the Mechanism of Interfacial Recognition[1]

Joseph P. Noel, Tiliang Deng, Kelly J. Hamilton, and Ming-Daw Tsai*

Department of Chemistry and Biochemistry Program
The Ohio State University, Columbus, Ohio 43210
Received January 17, 1990

We report substantial improvement in the catalytic potency of *bovine* pancreatic phospholipase A_2 (PLA2, overexpressed in *Escherichia coli*)[2,3] toward natural substrate phosphatidylcholine (PC) when Lys-56 was replaced by neutral amino acids, particularly methionine. As shown by the kinetic data summarized in Table I, the methionine mutant (K56M) shows a 4–5-fold increase in k_{cat} and a 4–5-fold decrease in K_m, and as a consequence, a 20–25-fold increase in k_{cat}/K_m for micellar dioctanoyl-PC (DC_8PC) and diheptanoyl-PC (DC_7PC) and monomeric dihexanoyl-PC (DC_6PC) and DC_7PC. Replacement of Lys-56 by other neutral amino acids Asn and Thr (K56N and K56T, respectively) also resulted in increased k_{cat} and decreased K_m, but to a smaller extent. Mutation to the positively charged Arg (K56R) resulted in very small changes.

Most, if not all, of the reported increases in k_{cat}/K_m for site-specific mutants were either for partial reactions or substrate analogues with lower activity (actually a change in substrate specificity).[4] The increase in k_{cat}/K_m for the K56M mutant should represent improved catalytic potency and is the largest reported to date, since DC_8PC micelle is the best natural substrate of bovine pancreatic PLA2. The highest k_{cat} observed for *bovine* K56M is even higher than that of the anionic substrate analogue DC_8-sulfate known to activate *porcine* PLA2.[5] Both k_{cat} and k_{cat}/K_m of K56M are comparable to those of dimeric snake venom PLA2 (Thr at position 56)[6] for DC_8PC micelles and are significantly higher for DC_6PC monomers[7] (see the last three rows of Table I). Crystal structural analysis by Sigler[6] suggested that one of the main causes for the higher catalytic efficiency of snake venom PLA2 is that the loop 57–66 (absent in dimeric snake venom enzymes) prevents the pancreatic enzyme from dimerization.[7] Recently Kuipers et al.[8] reported that deletion of this loop (Δ62–66) from *porcine* pancreatic PLA2 did result in en-

(1) For papers 1 and 2 in this series, see refs 2 and 3, respectively. This work was supported by Research Grant GM41788 from NIH. We thank Dr. R. L. Heinrikson for sharing the results in ref 11 prior to publication.

(2) Noel, J. P.; Tsai, M.-D. *J. Cell. Biochem.* **1989**, *40*, 309–320.

(3) Deng, T.; Noel, J. P.; Tsai, M.-D., submitted to *Gene*.

(4) (a) Takagi, H.; Morinaga, Y.; Ikemura, H.; Inouye, M. *J. Biol. Chem.* **1988**, *263*, 19592–19596. (b) Wilkinson, A. J.; Fersht, A. R.; Blow, D. M.; Carter, P.; Winter, G. *Nature* **1984**, *307*, 187–188. (c) Estell, D. A.; Graycar, T. P.; Miller, J. V.; Powers, D. B.; Burnier, J. P.; Ng, P. G.; Wells, J. A. *Science* **1986**, *233*, 659–663. (d) Wells, J. A.; Cunningham, B. C.; Graycar, T. P.; Estell, D. A. *Proc. Natl. Acad. Sci. U.S.A.* **1987**, *84*, 5167–5171. (e) Bone, R.; Silen, J. L.; Agard, D. A. *Nature* **1989**, *339*, 191–195.

(5) (a) Van Oort, M. G.; Dijkman, R.; Hille, J. D. R.; de Haas, G. H. *Biochemistry* **1985**, *24*, 7993–7999. (b) Volwerk, J. J.; Jost, P. C.; de Haas, G. H.; Griffith, O. H. *Biochemistry* **1986**, *25*, 1726–1733.

(6) Renetseder, R.; Brunie, S.; Dijkstra, B. W.; Drenth, J.; Sigler, P. B. *J. Biol. Chem.* **1985**, *260*, 11627–11634.

(7) Wells, M. A. *Biochemistry* **1974**, *13*, 2248–2257.

(8) Kuipers, O. P.; Thunnissen, M. G. G. M.; de Geus, P.; Dijkstra, B. W.; Drenth, J.; Verheij, H. M.; de Haas, G. H. *Science* **1989**, *244*, 82–85. Unlike DC_8PC, the k_{cat}/K_m for micellar DC_7PC is comparable between their deletion mutant and our K56M. Thus the effect of porcine Δ62–66 is more on altering substrate specificity.

0002-7863/90/1512-3704$02.50/0

Table I. Summary of Kinetic Data[a]

enzyme	substrate	state	k_{cat}, s^{-1}	K_m, mM	k_{cat}/K_m, M^{-1} s^{-1}
bovine WT	DC_8PC	micelles	675	1.4	0.48×10^6
K56M	DC_8PC[b]	micelles	2270	0.21	11×10^6
K56N	DC_8PC	micelles	1370	0.62	2.2×10^6
K56T	DC_8PC	micelles	1160	0.56	2.1×10^6
K56R	DC_8PC	micelles	510	0.75	0.68×10^6
bovine WT	DC_7PC	micelles	97	1.6	0.061×10^6
K56M	DC_7PC	micelles	420	0.35	1.2×10^6
bovine WT	DC_7PC	monomers	4.5	0.66	6.8×10^3
K56M	DC_7PC	monomers	13.5	<0.15	$>90 \times 10^3$
bovine WT	DC_6PC	monomers	2.4	4.9	0.49×10^3
K56M	DC_6PC	monomers	7.7	0.51	15×10^3
bovine WT	$DC_{12}PG$	micelles	600		
K56M	$DC_{12}PG$	micelles	330		
K56N	$DC_{12}PG$	micelles	170		
K56T	$DC_{12}PG$	micelles	170		
bovine WT	NOB	monomers	0.28	0.18	1.6
K56M	NOB	monomers	0.16	0.18	0.9
porcine WT	DC_8PC[c]	micelles	410	3.2	0.13×10^6
	DC_8-sulfate[d]	micelles	1340	0.21	6.4×10^6
porcine Δ62–66	DC_8PC[c]	micelles	980	1.9	0.51×10^6
porcine WT	DC_6PC[e]	monomers	0.9	6.0	0.15×10^3
C. atrox PLA2	DC_8PC	micelles	6350	0.18	35×10^6
C. adamanteus PLA2	DC_8PC[f]	micelles	4320	1.1	3.9×10^6
	DC_6PC[f]	monomers	1.6	4.0	0.40×10^3

[a] The data for bovine WT and mutants and *Crotalus atrox* PLA2 were produced in our laboratory while those for porcine and *Crotalus adamanteus* PLA2 were obtained from literature. Bovine PLA2 was isolated from an *E. coli* expression host BL21(DE3)plysS carrying a plasmid pTO-propla2[3] which contained a synthetic gene coding for bovine proPLA2.[2] The procedures for construction and purification of mutants will be described in detail in the future. The assays for PC substrates were performed at pH 8.0 (1 mM sodium borate, 25 mM $CaCl_2$, 100 mM NaCl) and 45 °C by using a pH stat method. The activities for $DC_{12}PG$ (mixed micelles) were determined at 5 mM PG, 15 mM deoxycholate, 5 mM $CaCl_2$, pH 8.0, 45 °C. The K_m of $DC_{12}PG$ cannot be determined since the system did not follow Michaelis–Menten kinetics. The assays for NOB were performed by a spectrophotometric method as described by Tomasselli et al.[11] [b] A k_{cat}/K_m value as high as 3×10^7 has been observed for this mutant, but decreased to 11×10^6 gradually in solution. The detailed cause is under investigation. [c] From ref 8. [d] From ref 5a. [e] From: Pieterson, W. A. Ph.D. Thesis, University of Utrecht, The Netherlands, 1973. Assays were conducted at pH 6.0 and 25 °C. [f] From ref 7.

hanced activity for micellar DC_8PC, but only a 2-fold increase in k_{cal} and a 2-fold decrease in K_m (also listed in Table I). For K56M, mutation of a single residue outside of the loop improves the catalytic potency of the bovine pancreatic PLA2 to comparable to that of dimeric snake venom PLA2. The mutant remains as a monomer as shown by gel filtration chromatography.

The structural basis of the enhanced catalytic potency remains to be established. Mechanistically, the results allow some clarification on the mechanism of "interfacial recognition" or "interfacial activation", which has been used to describe at least three activation phenomena related to PLA2: (a) the increased activity when substrate concenration exceeds its critical micelle concentration;[9] (b) the activation following the latency period often observed in monolayer assays;[10,11] and (c) the activation by anionic substrate surface as mentioned above for *porcine* pancreatic PLA2.[5] The mechanism remains highly controversial since many have equated the three phenomena and tried to explain all with a single mechanism.[12] Since K56M showed enhanced activity for *both* monomers and micelles, phenomenon a should be unrelated to Lys-56. Phenomena b and c could be related and involve Lys-56, as discussed below.

The choice of Lys-56 for the above studies was based on the recent report[11] that during the latency phase in the catalysis by porcine pancreatic PLA2 this residue is acylated by a substrate analogue, 4-nitro-3-(octanoyloxy)benzoate (NOB) monomers, as well as a natural substrate, dipalmitoyl-PC ($DC_{16}PC$) vesicles.[13] They also demonstrated that acylation resulted in dimerization of the enzyme and that the dimer is >100× more active (in relative activity) than the native PLA2 and suggested this process as the mechanism of "interfacial activation" of PLA2. Although their results are convincing, the level of acylation is far from being quantitative (16% of NOB and 3% for $DC_{16}PC$). Thus, it is likely that the enzyme activation following the latency period (phenomenon b) can be achieved in two mechanisms: acylation, as suggested by Tomasselli et al.,[11] and activation by the negatively charged fatty acid product[5] (phenomenon c). This is strongly supported by our observation that Lys-56 is involved in both.[14] The kinetic data of Lys-56 mutants agree that acylation of Lys-56 can activate the enzyme and suggest that the main function of acylation is charge neutralization. The same charge neutralization should be responsible for phenomenon c, since no improvement (indeed a small decrease) in the catalytic activity was observed for negatively charged substrates dilaurylphosphatidylglycerol ($DC_{12}PG$) and NOB (see data in Table I).

For PC substrates, the activation related to Lys-56 during the catalysis of wild type (WT) is apparently not optimal since both K56M and K56-acylated PLA2 have higher activity than WT. Other effects, such as hydrophobic interaction, could also con-

(9) (a) Wells, M. A. *Biochemistry* **1972**, *11*, 1030–1041. (b) Pieterson, W. A.; Vidal, J. C.; Volwerk, J. J.; de Haas, G. H. *Biochemistry* **1974**, *13*, 1455–1460.

(10) Verger, R.; Mieras, M. C. E.; de Haas, G. H. *J. Biol. Chem.* **1973**, *248*, 4028–4034.

(11) Tomasselli, A. G.; Hui, J.; Fisher, J.; Zürcher-Neely, H.; Reardon, I. M.; Oriaku, E.; Kézdy, F. J.; Heinrikson, R. L. *J. Biol. Chem.* **1989**, *264*, 10041–10047.

(12) Recent reviews: (a) de Haas, G. H.; Volwerk, J. J. *Lipid-Protein Interactions* **1982**, *1*, 69–149. (b) Dennis, E. A. *Enzymes* **1983**, *16*, 307–353. (c) Achari, A.; Scott, D.; Barlow, P.; Vidal, J. C.; Otwinowski, Z.; Brunie, S.; Sigler, P. B. *Cold Spring Harbor Symp. Quant. Biol.* **1987**, *52*, 441–452. (d) Jain, M. K.; Berg, O. G. *Biochim. Biophys. Acta* **1989**, *1002*, 127–156. (e) Waite, M. *The Phospholipases*; Plenum: New York, 1987.

(13) For *porcine* pancreatic PLA2, a lag phase was observed for PC but not for PG,[10] possibly because the latter can readily activate the enzyme. Some snake venom PLA2 did not show a lag phase,[10] and we also found that, unlike *porcine* PLA2, *bovine* PLA2 did not show a lag phase with NOB. How the extent of acylation is related to the latency period, the charge of substrates, and the structure of PLA2 from different sources are all interesting questions worthy of further investigation.

(14) Other lysines could also be involved in this or some other mode of activation, since de Haas showed that chemical acylation of the Lys-116 of porcine PLA2 and the Lys-10 of bovine PLA2 increased the penetrating power of the enzyme,[15] and Heinrikson showed that a monomeric snake venom PLA2 is acylated at both Lys-7 and Lys-10 by NOB.[16]

(15) (a) Van der Wiele, F. C.; Atsma, W.; Dijkman, R.; Schreurs, A. M. M.; Slotboom, A. J.; de Haas, G. H. *Biochemistry* **1988**, *27*, 1683–1688. (b) Van der Wiele, F. C.; Atsma, W.; Roelofsen, B.; van Linde, M.; Van Binsbergen, J.; Radvanyi, F.; Raykova, D.; Slotboom, A. J.; de Haas, G. H. *Biochemistry* **1988**, *27*, 1688–1694.

(16) Cho, W.; Tomasselli, A. G.; Heinrikson, R. L.; Kézdy, F. J. *J. Biol. Chem.* **1988**, *263*, 11237–11241.

tribute to the enhanced activity. Then, why would the native pancreatic PLA2 have Lys instead of Met at position 56? The problem could be related to substrate specificity. K56M is a better enzyme than WT for PC and under in vitro conditions, but not for negatively charged substrates PG or NOB. Since the physiological substrates of pancreatic PLA2 are negatively charged mixed micelles, the native pancreatic PLA2 should be as efficient as K56M physiologically. However, even for negatively charged substrates, it is unclear why pancreatic PLA2 would not have evolved to higher catalytic efficiency, as some snake venom PLA2 did under different physiological conditions.

Electron-Transfer Reaction of a Selenium Coronand–Copper(II) Complex. Formation of the Stable 1,5,9,13-Tetraselenacyclohexadecane Dication

Raymond J. Batchelor, Frederick W. B. Einstein, Ian D. Gay, Jian-Hua Gu, B. Mario Pinto,* and Xue-Min Zhou

Department of Chemistry, Simon Fraser University Burnaby, British Columbia, Canada V5A 1S6

Received January 9, 1990

We recently reported the synthesis and conformational analysis of selenium coronands.[1] These novel ligands could act as hosts for soft metal guests, and we proposed to test the importance of conformation on chelation. In addition, the rich redox chemistry exhibited by metal complexes of sulfur coronands[2] promised an exciting period of discovery with complexes of the heavier congeners. In particular, the preferential stabilization of lower oxidation states of metals was expected to be amplified with the third-row analogues. We report herein the first complex of a selenium coronand, namely, (1,5,9,13-tetraselenacyclohexadecane)copper(II) trifluoromethanesulfonate, $[Cu(16Se4)][SO_3CF_3]_2$ (**1**), and its spontaneous electron-transfer reaction in organic solvents to give Cu(I) as well as the intermediate radical cation $[16Se4]^{\bullet+}$ and the stable dication $[16Se4]^{2+}$. The salts $[(Cu(16Se4))_\infty]^{\infty+}([SO_3CF_3]^-)_\infty$ (**2**) and $[16Se4]^{2+}([SO_3CF_3]^-)_2$ (**3**) have been isolated from these solutions by selective crystallization. The complexes of Cu(II) with macrocyclic tetrathia ethers are stable, and the ligands are not oxidized.[3]

Complex **1**[4] (shown in Figure 1) is structurally[5] similar to the thia ether complex $[Cu(16S4)][ClO_4]_2$.[6] Both display square-planar coordination of Cu by the chalcogen atoms and have a

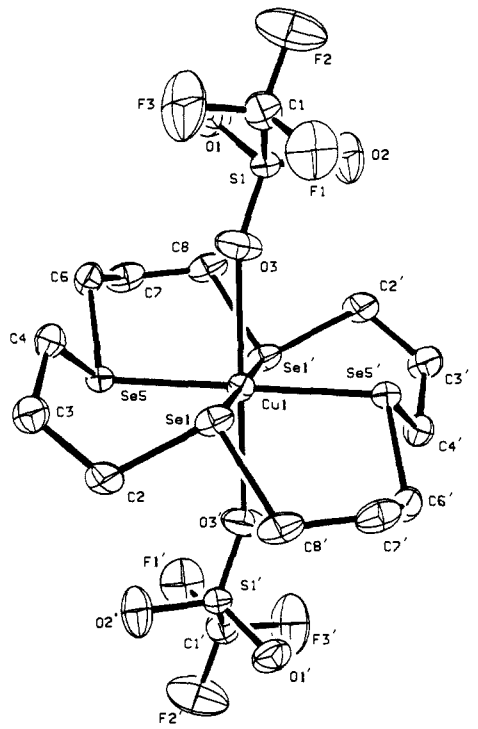

Figure 1. Molecular structure of $[Cu(16Se4)][CF_3SO_3]_2$ (**1**).

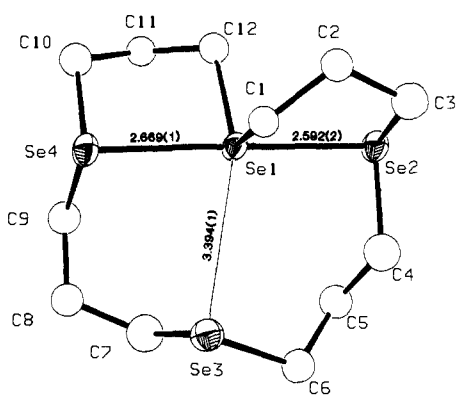

Figure 2. Molecular structure of the dication from $[16Se4]^{2+}([SO_3CF_3]^-)_2$ (**3**).

[4444] coronand conformation in which the chalcogen atoms occupy the central positions on the sides of the quadrilateral. Each anion coordinates much more weakly via one oxygen atom located on the pseudotetragonal axis of the complex (cf. sums of accepted covalent radii: Cu + Se, 2.54 Å; Cu + O, 2.11 Å). The Cu atom is located on a crystallographic center of inversion. The complex thus displays a tetragonally distorted octahedral arrangement typical of Cu(II).

Compound **1** is unstable in organic solvents such as CH_3CN, CH_3NO_2, $(CH_3)_2CO$, or THF. Indeed, prolonged reaction of 16Se4 and $Cu(CF_3SO_3)_2$ followed by precipitation with ether yielded colorless crystals of **2**.[4,7] A more detailed investigation of the electron-transfer process by UV-visible spectroscopy reveals the following salient features. The absorbance due to **1** at λ_{max} 466 nm in CH_2Cl_2 decays with a concomitant increase in the absorbance at λ_{max} 318 nm. This peak decays in turn and leads to the growth of an absorbance band at λ_{max} 223 nm. Analysis of the kinetic data from experiments performed at different concentrations of **1** and at different added-ligand concentrations indicates an initial rate that is first order in both complex **1** and ligand, and a mechanism for the reaction that is consistent with the following stoichiometry: $2[Cu^{II}(16Se4)]^{2+} + (16Se4) \rightleftharpoons$

* Author to whom correspondence should be addressed.

(1) Batchelor, R. J.; Einstein, F. W. B.; Gay, I. D.; Gu, J.-H.; Johnston, B. D.; Pinto, B. M. *J. Am. Chem. Soc.* **1989**, *111*, 6582.

(2) For recent references, see: Rorabacher, D. R.; Bernado, M. M.; Vande Linde, A. M. Q.; Leggett, G. H.; Westerby, B. C.; Martin, M. J.; Ochrymowycz, L. A. *Pure Appl. Chem.* **1988**, *60*, 501. Schroder, M. *Pure Appl. Chem.* **1988**, *60*, 517. Cooper, S. R. *Acc. Chem. Res.* **1988**, *21*, 141. Martin, M. J.; Endicott, J. F.; Ochrymowycz, L. A.; Rorabacher, D. B. *Inorg. Chem.* **1987**, *26*, 3012. Blake, A. J.; Gould, R. O.; Holder, A. J.; Hyde, T. I.; Schroder, M. *Polyhedron* **1989**, *8*, 513. Blake, A. J.; Gould, R. O.; Greig, J. A.; Holder, A. J.; Hyde, T. I.; Schroder, M. *J. Chem. Soc., Chem. Commun.* **1989**, 876.

(3) Gorewit, B. V.; Musker, W. K. *J. Coord. Chem.* **1976**, *5*, 67.

(4) Synthetic details, UV spectroscopic and microanalytical data for **1**–**3**, ^{77}Se CP-MAS solid state NMR data for **2** and **3**, and EPR data for **1** are given in the supplementary material.

(5) $[Cu(Se(CH_2)_3)_4][SO_3CF_3]_2$; monoclinic; $P2_1/n$; T = 190 K; a = 8.220 (2) Å; b = 10.965 (4) Å; c = 14.657 (5) Å; β = 105.44 (2)°; Z = 2; λ = 0.710 69 Å; μ(Mo Kα) = 67.49 cm^{-1}; crystal dimensions 0.15 × 0.31 × 0.43 mm; transmission 0.139–0.476, corrected analytically; $4° \le 2\theta \le 50°$; 1707 data ($I \ge 2.5\sigma(I)$); refined parameters, 152; $R = \sum||F_o| - |F_c||/\sum|F_o| = 0.037$; maximum |shift/error| ≤ 0.01. Bond distances: Cu(1)–Se(1), 2.4593 (6) Å; Cu(1)–Se(5), 2.4554 (6) Å; Cu(1)–O(3), 2.464 (5) Å; ⟨Se–C⟩, 1.96 Å. Bond angles: Se(1)–Cu(1)–Se(5), 88.40 (2)°; Se(1)–Cu(1)–O(3), 82.7 (1)°; Se(5)–Cu(1)–O(3), 90.1 (1)°.

(6) Pett, V. B.; Diaddario, L. L., Jr.; Dockal, E. R.; Corfield, P. W.; Ceccarelli, C.; Glick, M. D.; Ochrymowycz, L. A.; Rorabacher, D. B. *Inorg. Chem.* **1983**, *22*, 3661.

(7) Batchelor, R. J.; Einstein, F. W. B.; Gay, I. D.; Gu, J.-H.; Pinto, B. M. *Can. J. Chem.*, submitted.

0002-7863/90/1512-3706$02.50/0